Journal of the Earth and Space Physics, Vol. 42, No. 4, Winter 2017, PP. 13-26

Dynamics and thermodynamics analysis of tropical cyclone Haiyan

Pegahfar, N.[1*] and Ghafarian, P.[1]

1. Assistant Professor, Atmospheric Sciences Research Center, Iranian National Institute for Oceanography and Atmospheric Science, Tehran, Iran

(Received: 17 Oct 2015, Accepted: 18 Oct 2016)

Abstract

Tropical cyclone Haiyan (TCH) that formed over the West Pacific Ocean during 3-11 November 2013 has been investigated using three datasets of Japan Meteorology Agency, ECMWF and NCEP. Strength of TCH has been studied using two synoptic parameters of 10-m wind velocity and mean sea level pressure (MSLP). then, three dynamic parameters including vertical wind shear (VWSH) vector, helicity and potential vorticity (PV) together with the thermodynamic parameter of convective available potential energy (CAPE) have been calculated and analyzed during TCH life cycle. VWSH vector was analyzed in three classes of weak, moderate and strong shear, having northeasterly direction for most of TCH lifetime. Moreover, the helicity parameter was intensified to the tornadic instability (at about 6 hours later than the time of maximum 10-m wind speed), and its anomaly was located in the downshear quadrants for most of TCH life span. In addition, no significant PV anomaly was detected near TCH, but a subtropical PV anomaly was extended to the Philippines Islands before TCH eye reached this region. Also, CAPE parameter was intensified to strong instability class at about 48 hours earlier than the time of maximum 10-m wind speed and its anomaly was equally displaced in both up- and downshear quadrants. Finally, it can be concluded that 30-hourly lag between the time of CAPE maximum value and VWSH for which TCH was intensified to category 5.

Keywords: Tropical cyclone Haiyan, CAPE, Helicity, Potential vorticity, Vertical wind shear vector.

1. Introduction

Some energetic atmospheric systems with rotating motions have noticeable destructive effects on human life and their financial losses (Lee and Wurman, 2005). Meanwhile, recognition of causes of formation, intensification and weakening of tropical cyclone (TC) is of importance, especially on coastal regions. Hence, the relationship between this phenomenon and climate change has been intensively considered in the last decade (e.g., Chan and Liu, 2004; Chen, 2009; Emanuel, 2005; Webster et al., 2005; Fan, 2007a; Fan, 2007b; Shepherd and Knutson, 2007; Zhou et al., 2008). Also, many research studies from different aspects have been conducted to investigate TC using numerical weather prediction (NWP) (e.g. Ramalingeswara Rao et al., 2009), climate models (Camargo and Sobel, 2004) and also dense observational datasets. However, the last item still provides the best multi-scale analysis of TC. Some of variables and applicable approaches highlighting the importance of synoptic analysis in TC investigation are presented below:

(I) a pre-existing disturbance with sufficient amplitude in presence of air-sea interaction, which is a favorable condition for TC formation (Riehl, 1948; McBride and Zehr, 1981; Gray, 1968),

(II) Planetary Boundary Layer (PBL) parameters, affecting TC formation (Anthes and Chang, 1978),

(III) minimum central surface pressure related to SST between 26-30 ^{o}C (Titley and Elsberry, 2000),

(IV) break down of the mentioned relationship in item III for SST=30 ^{o}C (DeMaria and Kaplan, 1994),

(V) intrusion of very moist near-equatorial air into TC (Lajoie and Walsh, 2010),

(VI) angle of the equatorial air stream inflow (Lajoie and Walsh, 2010), and

[*]Corresponding author: E-mail: pegahfar@inio.ac.ir

(VII) vertical wind shear (Corbosiero and Molinari, 2003; Chen et al., 2006).

However, not only synoptic analysis of routine parameters (Barry and Carleton, 2001) but also dynamics (Kurgansky, 2008) and thermodynamic analysis (Molinari et al., 2012) should be considered in growth and development of a TC. Hence in the present work, three dynamic parameters including vertical wind shear (VWSH) vector, helicity and potential vorticity (PV) together with CAPE (Convective Available Potential Energy) as a thermodynamic parameter besides of some other routine synoptic parameters have been investigated during the life cycle of tropical cyclone Haiyan (TCH). This study covers generation, mature and dissipation processes of TCH. The rest of this paper has been arranged to describe theoretical basics (Sect. 2) and data and methods (Sect. 3). Following, case study of TCH is discussed in Sect. 4. Then, results and discussion together with conclusions are explained in Sect. 5 and 6, respectively.

2. Theoretical Framework

In this section, some characteristics of three dynamics parameters including VWSH, helicity and PV, together with thermodynamic parameter of CAPE are described, respectively.

(a) VWSH: this parameter, calculated using ($\vec{u}_{200} - \vec{u}_{850}$), is known as a factor with negative influence on TC intensity change at all stages of its lifetime (Gray, 1968; DeMaria and Kaplan, 1994; Hanley et al., 2001). Despite the uncertain nature of this parameter, its role has been investigated in (I) dry adiabatic dynamics (Raymond, 1992; Jones, 1995; Frank and Ritchie, 1999), and (II) idealized numerical models of TCs in creating azimuthal asymmetries of convection (DeMaria, 1996; Frank and Ritchie, 2001). Four general influences of VWSH on asymmetric vertical motion hypothesized by Jones (2000) have been listed as below:

(1) Since VWSH is accompanied by horizontal temperature gradient in balanced flow, vortex flow along environmental isentropes produces both downshear-upward motion and upshear-downward motion (Raymond, 1992; Jones, 1995).

(2) As VWSH begins to tilt the vortex, a compensating secondary vertical circulation is developed in an attempt to maintain the balanced flow. This circulation, which produces up- and downward motions in down- and upshear parts in that order (Raymond, 1992; Jones, 1995; DeMaria, 1996), acts to move the vortex back toward a vertical orientation. In the adiabatic framework, the secondary vertical circulation also creates potential temperature anomalies in the vortex, with a cold anomaly in downshear part and a warm anomaly in the upshear part of storm center.

(3) The isentropic flow along the vortex is distorted by VWSH and results in the upward motion to the right of the vertical tilt vector, which is initially downshear (Raymond, 1992). However, Jones (1995; 2000) demonstrated that vertical vortex interactions rotate its tilt vector away from downshear. Since upward motion is favored right of the tilt vector and the favored quadrant for upward motion also rotates with time.

(4) The last mechanism is appeared by the relative flow (the environmental flow minus the motion of the vortex) along the vortex isentropes associated with the warm core (Corbosiero and Molinari, 2002). The obtained pattern of this vertical motion depends on the vertical profiles of wind and potential vorticity in the vortex. This last mechanism is secondary to the second and third mechanisms discussed above.

(b) Helicity: Helicity is a standard factor of rotation in every point of a flow that corresponds to transfer of vorticity from environment to an air parcel in a convective motion. The concept of helicity, proposed by Betchov (1961), is suitable for prediction of extra-large cells with large and relatively long lasting helicity. This parameter is similar to curvature vorticity and depends on the angle between the direction and vorticity of the flow. The concept of helicity was used in meteorology by Angell et al. (1968) for the first time and defined as:

$$H = \int \overrightarrow{V_h} . \overrightarrow{\zeta_h} dZ = \int \overrightarrow{V_h} . \nabla \times \overrightarrow{V_h} dZ, \quad (1)$$

Using the horizontal components of wind velocity and vorticity ($\overrightarrow{V_h}$ and $\overrightarrow{\zeta_h}$, respectively) and Z as the height. Focusing on more than one fixed parameter is one of

helicity advantage, compared with vorticity parameter. The other main characteristic of helicity is that it can be served to quantify streamwise vorticity as a forecast tool for super-cell and tornado environment (Jones et al., 1990). Lilly (1986) pointed out that larger values of helicity prevent energy of flow from diffusing or scattering. Therefore, this concept can be applied in the investigation of intense convective storms and tornados, in which strong vertical motions exist and velocity and vorticity are aligned in the same direction. A turbulent fluid with large amount of helicity shows reluctance for transfer of energy to inertial range. Therefore, it can be inferred that small-scale atmospheric fluid with large amount of helicity is more stable and can be predicted more easily, compared with those with few amount of helicity.

According to some research studies, strength of rotating phenomenon is related to the helicity value (Davies, 2006; Weisman and Rotunno, 2000) that is estimated at the standard fixed layer of 0-1 or 0-3 km (Rasmussen and Blanchard, 1998). However, Thompson et al. (2007) showed that estimation of helicity using inflow layer, discriminates between significantly tornadic and non-tornadic super-cell comparing with standard fixed layer version of helicity. Table 1 shows a list of categorized values of helicity according to various instabilities.

It should be noted that TC itself provides the environmental helicity for its individual cells (Molinary and Vollaro, 2008). Also, Khansalari et al. (2011) investigated the applicability of helicity during cyclone Gonu and showed that dynamic buoyancy was the main factor in producing helicity.

(c) Potential Vorticity (PV): PV as a quantity that is proportional to the dot product of vorticity and stratification, is a useful concept for understanding generation of vorticity in cyclogenesis, analyzing oceanic flows and tracing stratospheric air in the troposphere. This concept was formulized by Rossby (1940) and developed by Ertel (1942) as:

$$PV = \frac{1}{\rho}\zeta_a.\nabla\theta, \quad (2)$$

where θ is potential temperature, ζ_a (containing Coriolis parameter of $f = 2\Omega\ sin\ (\varphi)$) is the absolute vorticity and ρ is the fluid density. To study PV generation due to latent heat release and elimination of friction effect on PV calculation, this parameter is generally considered at 300 hPa and 700 hPa pressure levels, respectively.

(d) Convective Available Potential Energy (CAPE): CAPE is the amount of energy that an air parcel should have to be able to pass a special distance vertically in the atmosphere. This parameter is actually the positive buoyancy of an air parcel and shows the sign of stability or instability condition of the atmosphere. Hence, CAPE plays a key role in numerical weather predictions. The value of CAPE can be calculated via the below equation

$$CAPE = \int_{z_{LFC}}^{z_{EL}} g\left(\frac{T_{v,\,parcel} - T_{v,\,env}}{T_{v,\,env}}\right) dz. \quad (3)$$

Where z_{LFC} is the free convection level height, z_{EL} is the balance level height (neutral buoyancy), $T_{v,\,parcel}$ is the virtual temperature of air, $T_{v,\,env}$ is the virtual temperature of environment and g is the gravitational acceleration. A list of stability and instability stratifications corresponding to CAPE values are shown in Table 2.

Table 1. Relationship between helicity and instability of the atmosphere (From http://www.theweatherprediction.com/habyhints/313/)

Helicity (J/kg or m^2/s^2)	Instability
150 < H < 299	Supercells possible with weak tornadoes according to Fujita scale
300 < H < 450	Very favorable to supercells development and strong tornadoes
450 < H	Violent tornadoes when calculated only below 1 km (4,000 feet), the cut-off value is 100

Table 2. CAPE values correspond to various atmospheric instabilities (From http://www.tornadochaser.net/cape.html)

CAPE values (J/kg or m^2/s^2)	Stability-instability
CAPE < 0	Stable
0 ≤ CAPE < 1000	Low instability
1000 ≤ CAPE < 2500	Moderate instability
2500 ≤ CAPE < 4000	Intensive instability
4000 ≤ CAPE	Extreme instability

3. Data and methods

In the current paper, two sets of re-analysis data have been used including (I) GFS-ANL data with 0.5° × 0.5° spatial resolution at 26 vertical pressure levels, and (II) ECMWF-ERA interim data with 0.75° × 0.75° latitude–longitude horizontal resolution at 37 pressure levels, both with 6-hourly time intervals. To focus on the selected area, data have been analyzed over 100-160 °E and 0-30 °N. Moreover, a dataset from local stations produced by Japan Meteorological Agency (JMA) have been used.

To calculate values of the considered parameters in TCH eye, the values from the nearest grid points to TCH eye have been selected. Also at each time, data from a square domain of 5°×5° centered by TCH eye have been excluded to find the maximum values of the considered parameters. In addition, radial extend of up- and downshear around a TC, introduced by Corbosiero and Molinari (2002) (Figure 1), has been used to address different direction around TCH.

VWSH has been computed via (1) using the formula of $u_{200} - \vec{u}_{850}$, (2), applying the method defined by Stevenson et al. (2014), and (3) averaging values in a radius of 500 km, determined by a square of $5^o \times 5^o$ including 10 grid points in each direction, respectively.

4. Case study: TCH

TCH was one of the strongest storms over the West Pacific Ocean and affected the south-east part of Asia, especially the Philippines Islands. Figure 2a and b show TCH track and the time evolution of its intensity. This storm was generated from a region of low pressure in the southeast of Pohnpei in the Federated States of Micronesia on the last hours of 2 November 2013 and reached the Philippines region with the speed of 76.38 m/s on 7 November 2013. Based on the records, TCH was the most lethal typhoon over the Philippines Islands and developed to a super storm thorough its westerly motion. It killed about 6300 people and caused 1785 missing and 2.86 billion USD of property damages. TCH ultimately reached the northern part of Vietnam on 10 November 2013 and continued its activity until 12 November 2013, when entering the south-east coast of Asia.

5. Results and discussion

Before presenting the dynamic analysis of TCH, it is worthwhile to emphasize TCH intensity using some routine synoptic variables. Hence, the parameters of 10-m wind velocity and mean sea level pressure (MSLP) are analyzed in Sect. 5.1 and then dynamics and thermodynamics analysis are presented in Sect. 5.2.

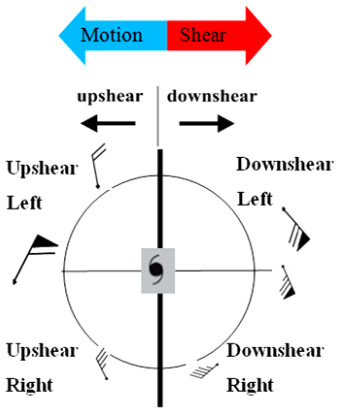

Figure1. Radial extend of up- and downshear quadrants around a TC, taken from Figure 3 in Corbosiero and Molinari (2002). To show the wind shear direction, results from Molinari and Vollaro (2008) have been also added to the diagram.

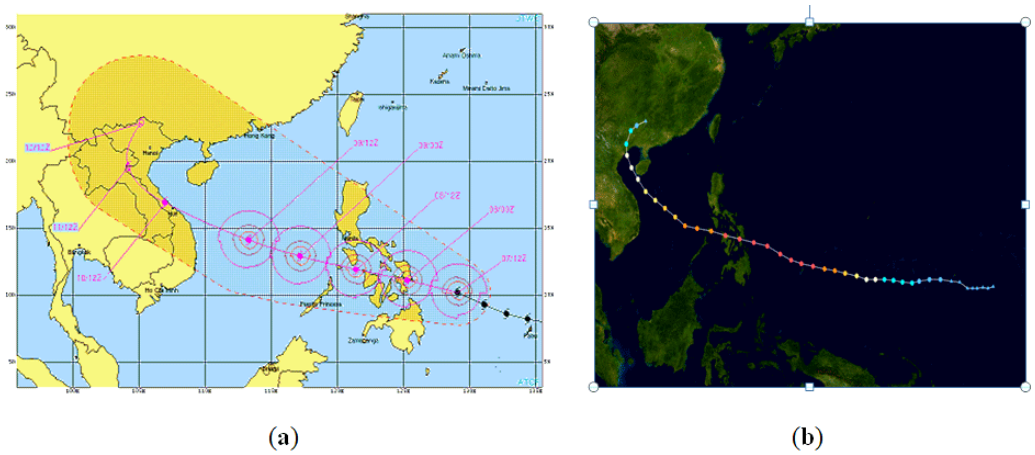

Figure 2. (a) Track of TCH during 3-12 November 2013 and (b) the intensity of storm in 6-hourly intervals as colored points, taken from (http://www.weather.gov.hk/wxinfo/currwx/tc_prevpos_1339.html)

5.1. Synoptic analysis

5.1.1. Wind velocity and pressure

Two variables of 10-m wind velocity and MSLP have been studied from 3-11 November 2013 at TCH eye and eyewall. Horizontal distributions of these two variables are shown in Figure 3. Red circle in all subplots shows TCH eye location. TCH intensification can be deduced from the comparison of the right and left columns in Figure 3. Increase of anti-cyclonic curvature of wind field (Figure 3a and b) and also the horizontal gradient of MSLP (Figure 3c and d) reveal that TCH peak activity occurred on 7 November 2013. Moreover, the westward motion of TCH can be seen in Figure 3.

To elucidate the TCH intensity, Figure 4 was plotted using data measured at some local stations. This Figure shows time series of maximum wind speed in TCH eyewall (Figure 4a) and the minimum pressure in TCH eye (Figure 4b) during TCH lifetime, both are based on Saffir–Simpson classification. Figure 4 shows that TCH was in category 5 for 2 days. Also, simultaneous occurrence of maximum wind speed and minimum pressure can be seen from this figure with inverse behavior of increasing/decreasing trends.

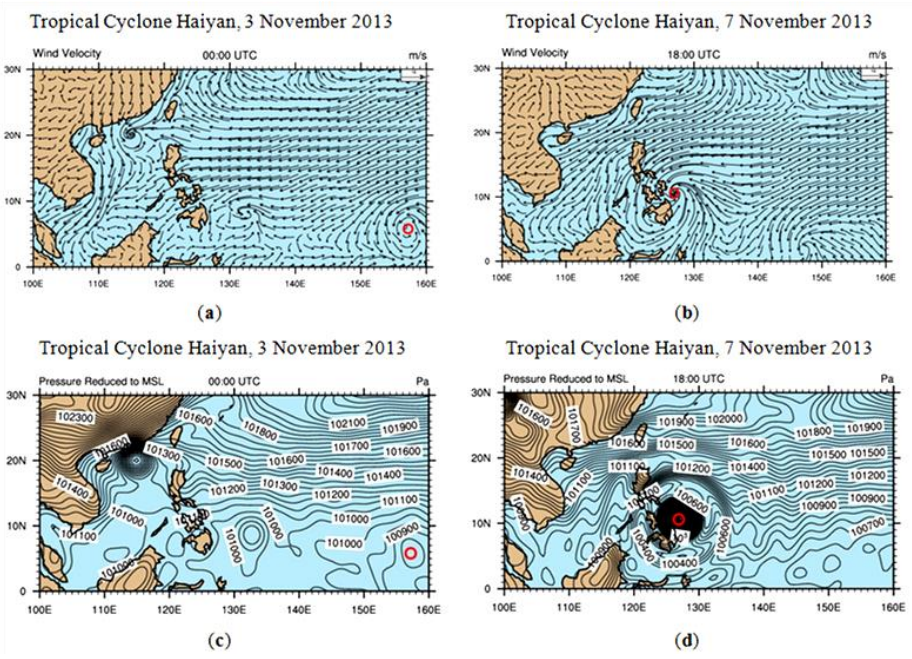

Figure 3. Horizontal patterns of 10-m wind velocity and pressure reduced to mean sea level at 0000 UTC 3 November 2013 (a and c) and 1200 UTC 7 November 2013 (b and d). The red circle in each subplot shows TCH eye location.

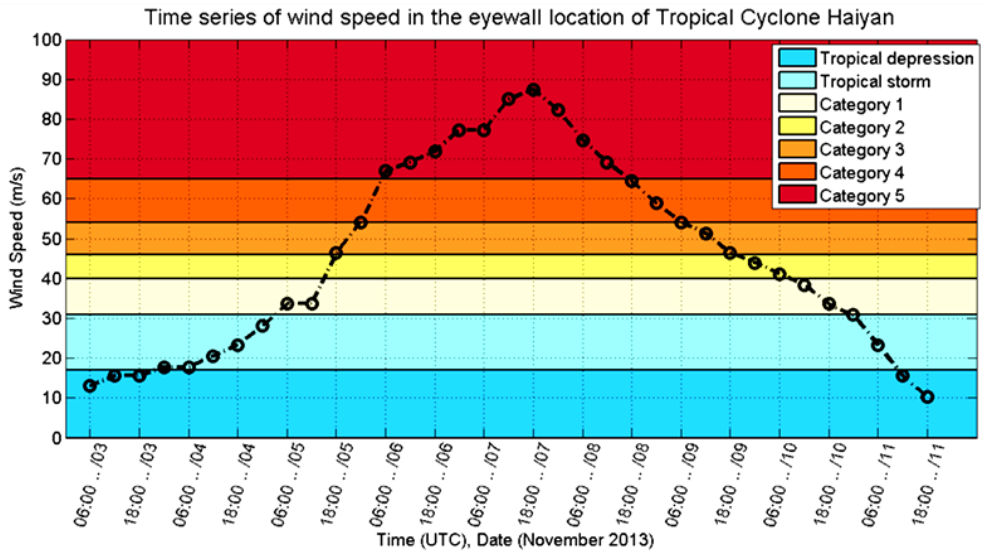

(a)

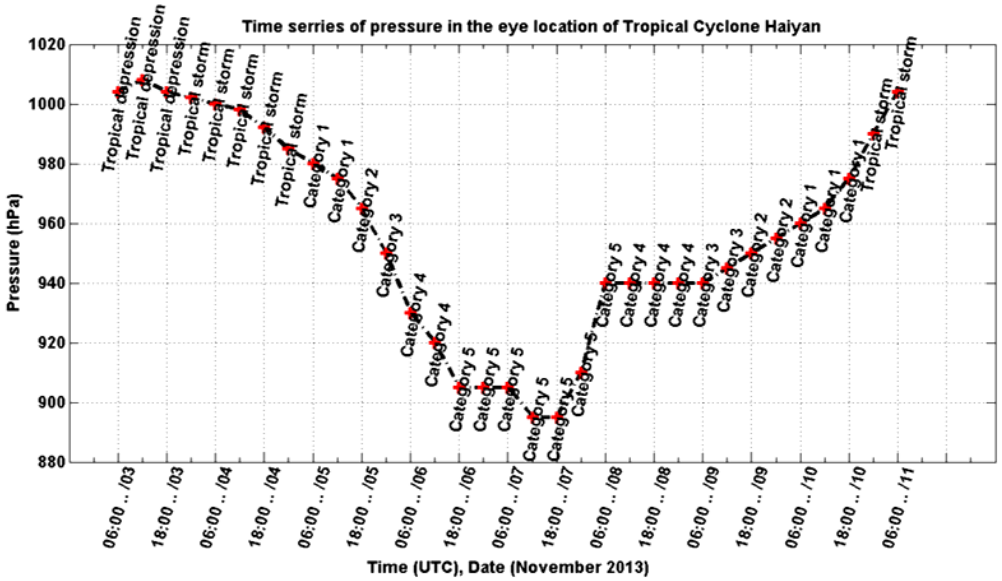

(b)

Figure 4. Time series of maximum 10-m wind speed (a) and minimum pressure (b), using JMA data. Colored layer in (a) was depicted based on Saffir–Simpson categories denoted in the legend. Classification of TC intensity for pressure is superimposed on each point in (b).

5.2. Dynamics and thermodynamics analysis

5.2.1. VWSH vector

Time series of VWSH in TCH eye has been calculated using the relation of $\vec{u}_{200} - \vec{u}_{850}$ and plotted in Figure 5. According to Corbosiero and Molinari (2002) findings, three classes for VWSH including weak (VWSH< 5 m/s), moderate (5 m/s < VWSH < 10 m/s) and strong (VWSH > 10 m/s) classes have been demonstrated in Figure 5 indicating the frequency of 5%, 17% and 78%, respectively. It is clear that the strong class of VWSH around TCH eye location reached maximum value of 45 m/s. Also, the averaged values of VWSH in a square domain of $5^o \times 5^o$ around TCH eye location have been calculated based on the method defined by Stevenson et al. (2014) for each time step. The results are shown as the yellow bars in Figure 5. Frequency of the averaged values of VWSH in weak, moderate and strong classes, is 36%, 53% and 11%, respectively.

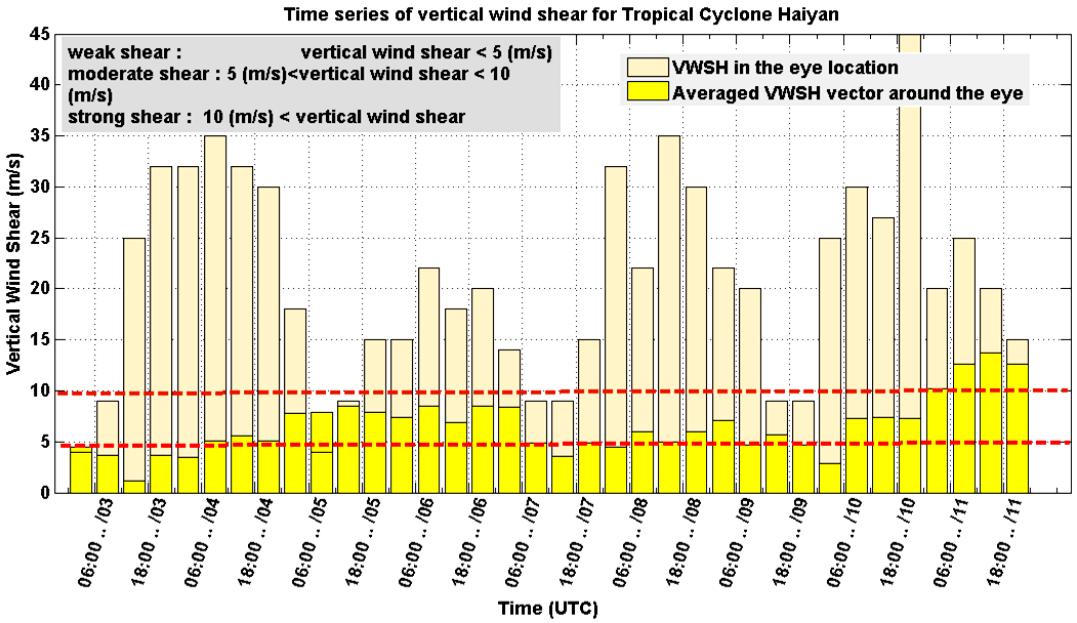

Figure 5. Time variation of VWSH calculated in TCH eye location (cream bars) and the averaged values of VWSH over a $5^o \times 5^o$ square domain around TCH eye (yellow bars). Two horizontal dashed lines demonstrate metrics defined by Corbosiero and Molinari (2002) as indicated in the legend.

The direction change of VWSH vector, during TCH life cycle, is shown in Figure 6. Analysis of VWSH vector magnitude (Figure 6a) shows that shear value is minimum at the beginning of TCH life (3 November 2013), then is maximized during 2 days (at the end of 5 November 2013), afterward decreased until the end of 9 November 2013, and again is increased from the beginning of 10 November 2013. Increasing and decreasing trends of VWSH is opposite to the TCH intensification trend.

Figure 6b shows the directional abundant of VWSH vector and indicated that the most of the shear vectors belong to the 180-240° sector. Also, Figure 6b implies that the direction of VWSH vectors do not always aligned 180° opposite to the TCH motion direction.

Moreover, the latitudinal - longitudinal pattern of VWSH vectors for TCH is shown in Figure 7. The rotational nature of VWSH vector around TCH eye can be easily seen, which is due to vortex interactions in the vertical and leads to a rotation of tilt vector away from downshear (Jones, 1995; 2000).

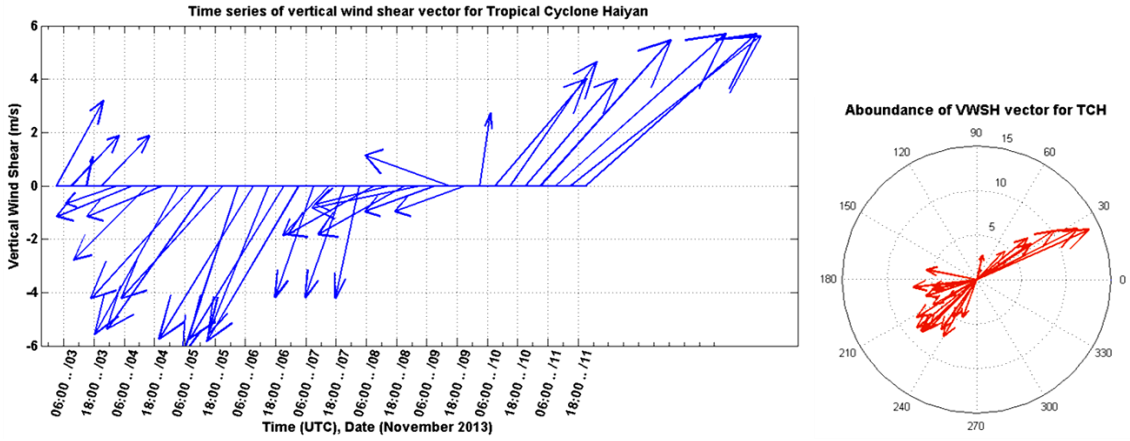

(**a**) (**b**)

Figure 6. Time series (a) and directional abundant (b) of VWSH vector during TCH life cycle.

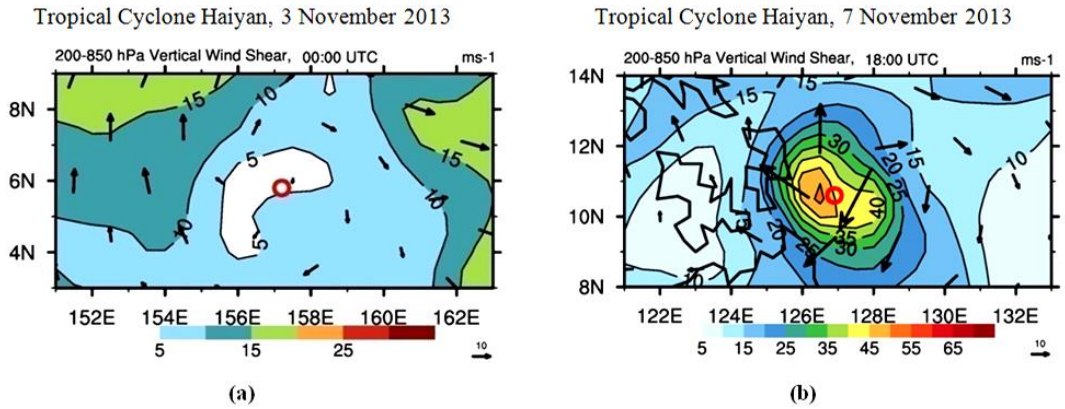

Figure 7. Latitudinal - longitudinal distribution of VWSH vector at 0000 UTC 3 November 2013 (a) and 1800 UTC 7 November 2013 (b). The shaded patterns show the VWSH magnitude and the reference arrow of 10 m/s has been show in the lower part of each subplot. The red circle shows TCH eye location in each subplot.

5.2.2. Helicity

Time series of helicity values in TCH eye and eyewall is depicted in Figure 8. In this figure, values of helicity in TCH eye could not reached the possible supercell class, except at 0000 UTC 6, 0600 UTC 7 and 10 November 2013 when the helicity exceeded 150 J/kg or m^2/s^2 value at the nearest grid point to TCH eye. This can be referred to the shrink of TCH eye so that the nearest grid point could not be a representative of the eye. This inaccuracy occurred due to the poor horizontal resolution of the data.

Time variation of maximum values of helicity, occurred out of TCH eye location, and is depicted by solid thick line in Figure 8. It can be easily seen that at 0000 UTC 8 November 2013, helicity was maximized (around 2000 J/kg value). Figure 8 also shows that TCH was strengthened to the tornadic supercell class and maintained in this class for more than 102 hours, initiated from 1200 UTC 5 November 2013 and continued until the end of TCH lifecycle. Gaining the great value of 2000 J/kg for helicity clearly implies that TCH should stand for a long time according to the results reported by Droegemeier et al. (1993). They showed that storms formed in environments characterized by large helicity are longer-lived than those in less helical surroundings. To show the maintenance and propagational characteristics of TCH based on helicity parameter, as mentioned by Weisman and Rotunno (2000) for other TCs, the horizontal patterns of helicity are plotted for the whole of TCH lifetime. The results are depicted for 3, 5, 7, 8 and 11 November 2013 in Figure 9. Helicity values of around 25 J/kg (at 0600 UTC 3 November 2013, Figure 9a) was increased to a value of around 300 J/kg (at 1800 UTC 5 November 2013, Figure 9b). As Figure 9c shows helicity was strengthened and reached more than 550 J/kg value at 1800 UTC 7 November 2013. The horizontal gradient of helicity reveals the TCH intensity as well (Figure 9d). At the end of TCH life span, the helicity value in TCH environment was decreased to less than 300 J/kg, which was simultaneous with the formation of a new helicity anomaly at the southeast of TCH. The new helicity anomaly was strengthened to 550 J/kg value and reached near the TCH eye through 12 hours.

Results of applying the radial extend standard, defined by Corbosiero and Molinari (2002) (Figure 1) together with the obtained VWSH vector direction for TCH show that the first environmental helicity anomaly was formed in the upshear part and continued in downward half of TCH. Also helicity anomalies was laid in the left quadrants at the peak activity time of TCH (7 and 8 November 2013). At 1800 UTC 9 November 2013, helicity anomaly was entirely shifted to the downshear quadrants. At the end of TCH life cycle, it slowly moved to the right-downshear quadrant. It is worthwhile to note that our findings are similar to Molinari and Vollaro (2008) results, as the maximum helicity value occurred in the downshear-left quadrant for Hurricane Bonnie (1998).

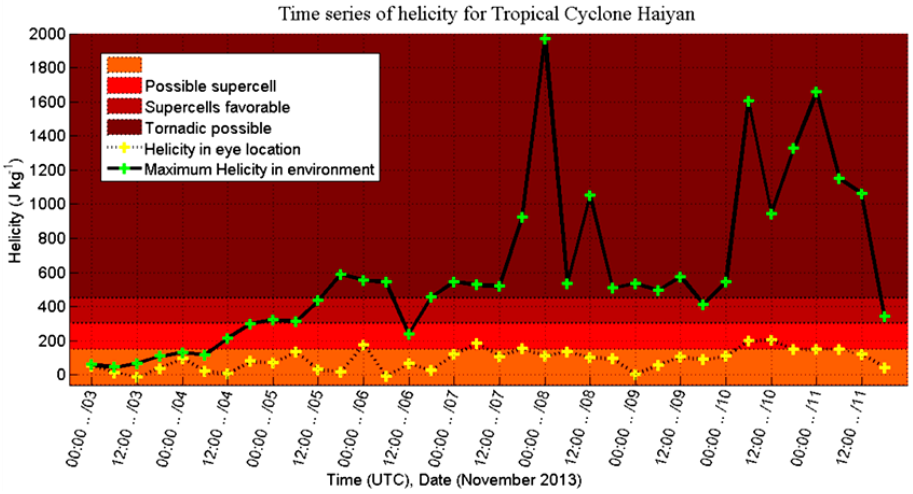

Figure 8. Time series of helicity (J/kg) in TCH eye (dotted line) and the maximum values occurred in its environment (solid line). Colored layers show the relationship between the corresponding parameter and storm instability classification, defined in the legend.

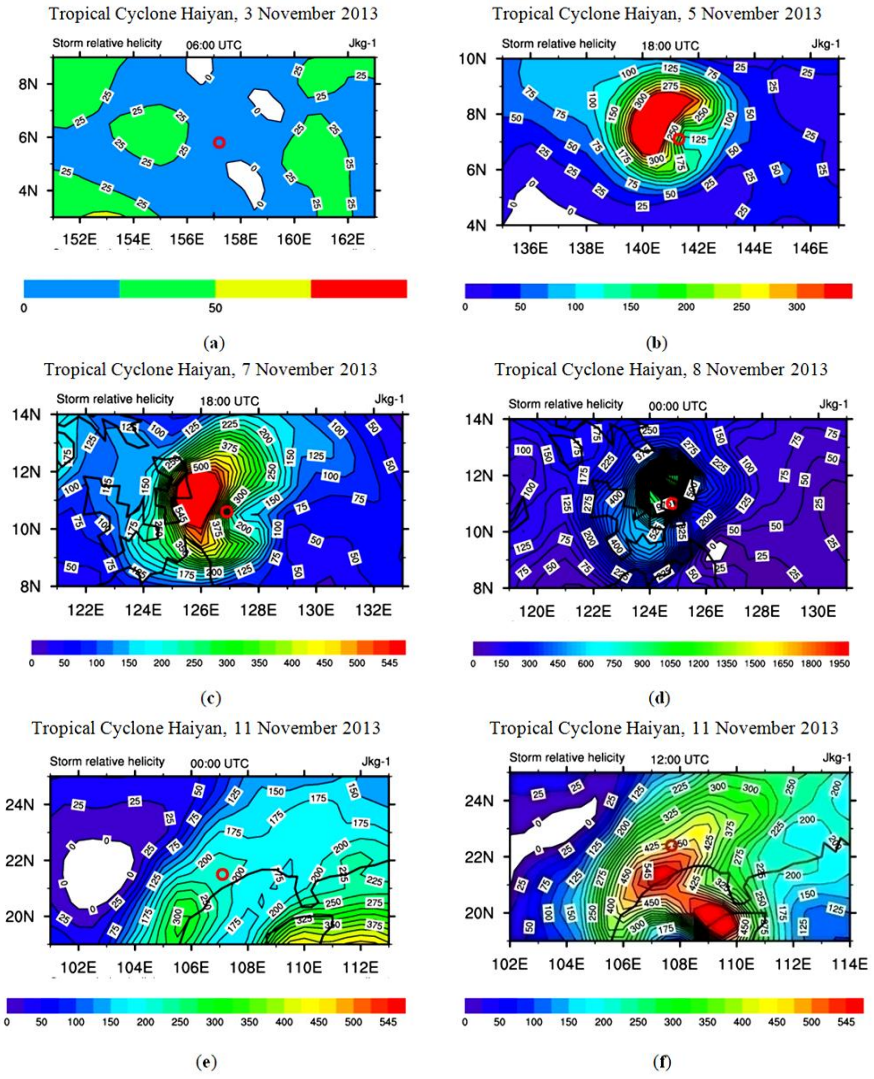

Figure 9. Horizontal patterns of helicity (J/kg) during TCH lifetime, at 0600 UTC 3 November (a), 1800 UTC 5 November (b), 1800 UTC 7 November (c), 0000 UTC 8 November (d), 0000 UTC 11 November (e) and 1200 UTC 11 November 2013 (f). Red circle in all panels demonstrates the eye location. Color bar has been shown in the lower part of each subplot.

5.2.3. PV

The horizontal patterns of PV were calculated at two pressure levels of 300 and 700 hPa and are plotted for 7 and 9 November 2013 (Figure 10). Results indicate that because of the TCH location in the lower latitudes (near equator and with near zero value of Coriolis parameter) no significant PV was detected near TCH, at neither 300 hPa nor 700 hPa. Only a subtropical PV anomaly affected TCH passing the equatorial latitude (< 8 ^{o}N) and reaching subtropical region. On the 7 of November 2013 and at 300 hPa level, a subtropical PV anomaly with negative values was extended to the Philippines Islands before TCH eye reached this region (Figure 10a), and it was diminished on 9 November 2013. At 700 hPa, a subtropical negative PV anomaly can be seen over the coast of Vietnam both on 7 and 9 of November 2013.

5.2.4. CAPE

Time series of the thermodynamic parameter CAPE (taken from GFS reanalysis data) is plotted in TCH eye (Figure 11). Also maximum values detected in the environment of TCH was added to this figure. Regarding the instability classes defined for CAPE parameter, the values of CAPE in the TCH environment belong to the moderate and strong instability classes, except for two values that occurred in the last day that corresponded to the weak instability class. The values of CAPE, at the nearest grid point to TCH eye location, never reached the strong instability classes, as a calm weather expected for the eye. The intrusion of CAPE values into the moderate instability class, at the nearest grid point to the TCH eye location, may be due to the intensification of TCH and shrinking TCH eye. So, the CAPE values may be used to delete the eye location. Clarification for this due to poor resolution of the reanalysis data, that is not possible without numerical simulations. Achieving the value of not more than 3500 J/kg for CAPE shows that TCH was not intensified to the extreme instability class. Out of TCH eye location, the maximum values of CAPE experienced a frequency of 5% in a week, 61% in moderate and 33% in strong instability classifications.

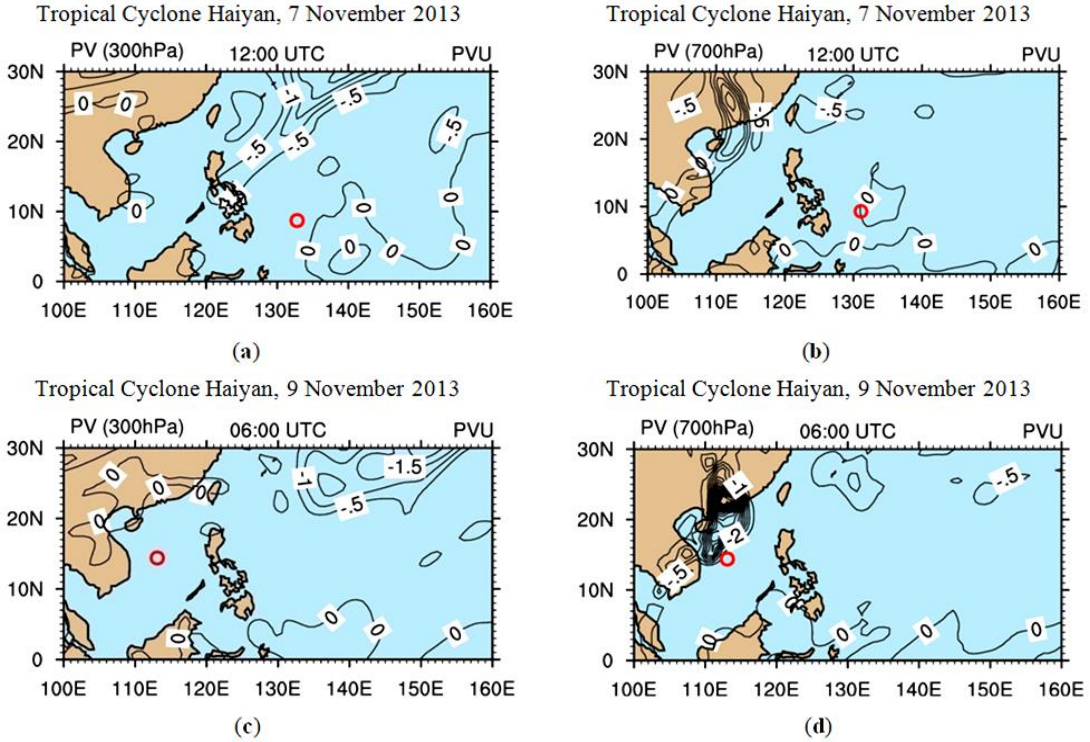

Figure 10. Horizontal patterns of PV (PVU) during TCH life cycle at 1200 UTC 7 November 2013 (a and b) and at 0600 UTC 9 November 2013 (c and d). Left column depicts PV at 300 hPa and the right one shows that for 700 hPa. Red circle in each panel demonstrates TCH eye location.

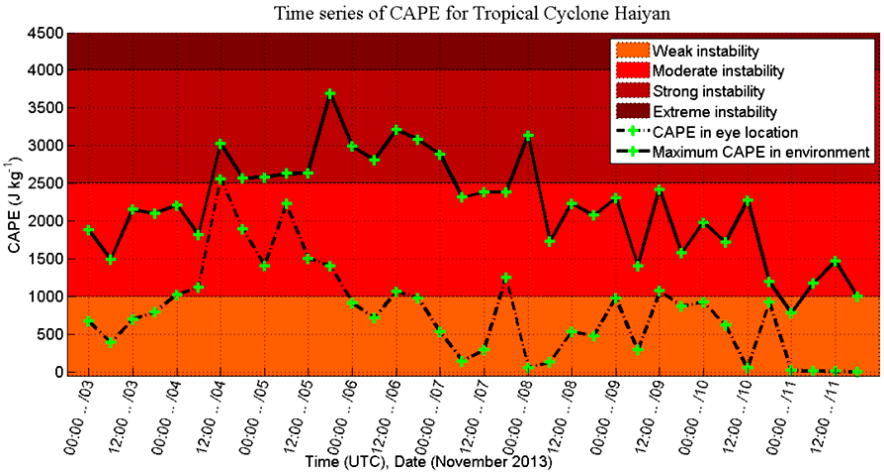

Figure 11. Time series of CAPE parameter (J/kg) in TCH eye location (dotted line) and also the maximum values out of TCH eye location (solid line). Colored layers show the corresponding instability classifications defined in the legend.

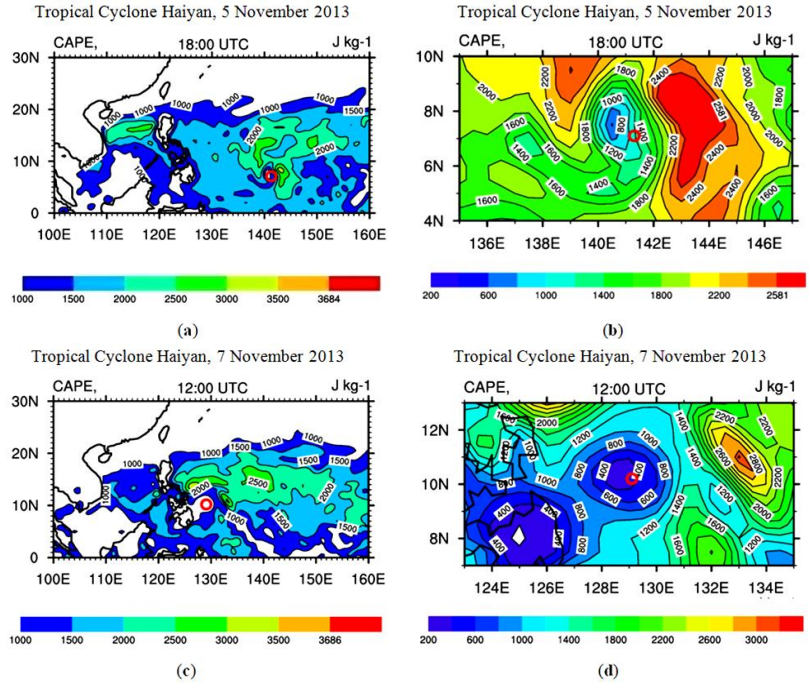

Figure 12. Horizontal patterns of CAPE (J/kg) during TCH on 1800 UTC 5 November 2013 (a, b) and 1200 UTC 7 November 2013 (c, d). The right column has been prepared as the zoom of the left column. Red circle in all panels demonstrates TCH eye location. Color bar has been shown in the lower part of each subplot.

The horizontal patterns of CAPE for TCH is plotted for 5 and 7 November 2013 in Figure 12. A CAPE anomaly existed in the northwest of TCH eye at the beginning of its lifetime with a clear distance between them until 5 November 2013. Two days later, on 7 November 2013, TCH eye passed the CAPE anomaly (values less than 1000 J/kg) and after 24 hours it was entirely positioned in the west part of the CAPE anomaly. Near zero values of CAPE on 8 and 10 November 2013 is remarkable. Such low values refer to the stop time for vertical motions and means that no feeding occurred from the oceanic surface layer.

One of the other remarkable points is equally positioning of CAPE anomaly in the both upshear and downshear quadrants. Our findings support the hypothesis argued by Corbosiero and Molinari (2002) for convectively active tropical cyclones, as a deep divergent circulations oppose the vertical wind shear and act to minimize the tilt. This allows maximum convection to remain without rotating with time. However, Molinari and Vollaro (2010) indicated that

CAPE in strongly sheared storms was 60% larger in downshear. Also Molinari and Vollaro (2008) examined the spatial variation of CAPE in Hurricane Bonnie (1998) and concluded that the mean value of CAPE was also 3 times larger in downshear.

6. Conclusion

In this research, the TCH as the strongest TC formed over the West Pacific Ocean until 2014 was analyzed using some synoptic, dynamics and thermodynamic parameters. For this aim, three sets of JMA, ECMWF and GFS-NCEP were used for the period of 3-12 November 2013. JMA dataset was measured at some local stations while the last two datasets are included in the reanalysis data with the horizontal resolution of $0.75^o \times 0.75^o$ and $0.5^o \times 0.5^o$, respectively. For data processing, two parts including eye and eyewall were defined for TCH in 6-hourly time intervals. Also an averaging method defined by Corboseiro et al. (2002) was applied to determine the VWSH vector at each time step.

Intensity of the selected TC, using the synoptic parameters of 10-m wind velocity and MSLP were analyzed that showed intensification of TCH to category 5, based on Saffir-Simpson scales. Simultaneous occurrence of the maximum wind speed (~value of 90 m/s) and the minimum surface pressure (~ 895 hPa) were recorded at 1800 UTC 7 November 2013. Then the dynamics parameters of VWSH, helicity and PV were investigated. The obtained results are itemized as below:

(1) TCH experienced all three classes of weak, moderate and strong VWSH during its life cycle. The maximum value of VWSH occurred at 0000 UTC 7 November 2013. Also VWSH vector, computed over a $5^o \times 5^o$ square domain centered by TCH eye, had the values of 36%, 53% and 11% for the above three VWSH intensity classes, respectively. Also, the dominant direction for VWSH was northeasterly during TCH period. The higher frequency of moderate class of VWSH supports Nolan and McGauley (2012) findings as the positive role of VWSH in facilitating TC formation and development.

(2) Helicity values during TCH reached a value of 2000 J/kg and was laid in the favorable supercell class. Also, the helicity anomaly was located in the downshear quadrants at most of the TCH lifetime. According to the helicity time series, this parameter was maximized at 0000 UTC 8 November 2013, at around 6 hours later than TCH maximum activity time.

(3) No significant value of PV was seen; neither at 300 hPa nor at 700 hPa. However, a subtropical PV anomaly with negative value (at 300 hPa level) extended to the Philippines Islands before TCH eye reached this area. So, it could be concluded that accompanying the subtropical PV anomaly together with TCH effects increased the severe weather conditions over the Philippines Islands.

Moreover, CAPE analysis showed that this parameter was not strengthened to the extreme instability class during TCH period and only gained around 3500 J/kg value. Also during TCH life cycle, the CAPE anomaly was located at upshear and downshear quadrants equally, while Molinari and Vollaro (2008 and 2010) introduced 60% larger values in downshear part. As the other remarkable point, CAPE was maximized at about 48 hours earlier than TCH peak activity time. The observed lag between the time of CAPE and helicity maximum values (about 54 hours) can be interpreted as this fact that updraft motion should be intensified firstly and then rotation could be strengthened. Therefore, it could be acclaimed that this lag between the time of CAPE and helicity maximum values is one of the TCH characteristics. In spite of CAPE cease for intensive instability class and not reaching extreme instability class, decreasing/increasing trend of pressure/wind speed continued for 48 hours.

Finally, our findings showed that there was an inconsistency between various metrics of the TC classifications during TCH life cycle. So 30-hourly lag between occurrence of CAPE and VWSH maximum values could be interpreted as one of the probable reasons for TCH intensification to category 5. Hence, it can be concluded that the total synoptic, dynamics and thermodynamic parameters together with their dominance hierarchy influences on TC should be focused on to access a vast feature and description of a TC. Focusing on these various parameters in terms of horizontal distribution and time series allows the

evolution of TS_s to be investigated using meteorological tropical cyclone models.

Acknowledgements The authors are thankful to the Iranian National Institute for Oceanography and Atmospheric Science, Tehran, Iran for their financial support for this research (project No. 393-033-01) and ECMWF and NCEP-GFS teams for providing re-analysis data. The authors would like to thank Dr. Maryam Gharaylou for her insightful review.

References

Angell, J. K., Pack, D. H. and Dikson, C. R., 1968, A Lagrangian study of helical circulation in the planetary boundary layer, J. of Atmos. Sci., 24(5), 707-717.

Anthes, R. A. and Chang, S. W., 1978, Response of the hurricane boundary layer to changes of sea surface temperature in a numerical model, J. Atmos. Sci., 35, 1240-1255.

Barry, R. G. and Carleton, A. M., 2001, Synoptic and dynamic climatology, Psychology Press.

Betchov, R., 1961, Semi-isotropic turbulence and helicoidal flows, Phys. Fluids, 4, pages 925.

Camargo, S. J. and Sobel, A. H., 2004, Formation of tropical storms in an atmospheric general circulation model, Tellus, 56(A), 56-67.

Chan, J. C. L. and Liu, K. S., 2004, Global warming and western North Pacific typhoon activity from an observational perspective, J. Climate, 17(23), 4590-4602.

Chen, S. S., Knaff, J. A. and Marks Jr. F. D., 2006, Effects of vertical wind shear and storm motion on tropical cyclone rainfall asymmetries deduced from TRMM, Mon. Wea. Rev., 134, 3190-3208.

Chen, G. H., 2009, Inter decadal variation of tropical cyclone activity in association with summer monsoon, sea surface temperature over the western North Pacific, Chinese Science Bulletin, 54(8), 1417-1421.

Corbosiero, K. L. and Molinari, J., 2002, The effects of vertical wind shear on the distribution of convection in tropical cyclones, Mon. Wea. Rev., 130, 2110-2123.

Corbosiero, K. L. and Molinari, J., 2003, The relationship between storm motion, vertical wind shear, and convective asymmetries in tropical cyclones, J. Atmos. Sci., 60, 366-376.

Davies, J. M., 2006, Tornadoes in environments with small helicity and/or high LCL heights, Weather and forecasting, 21(4), 579-594.

DeMaria, M. and Kaplan, J., 1994, Sea surface temperature and the maximum intensity of Atlantic tropical cyclones, J. Climate, 7, 1324-1334.

DeMaria, M., 1996, The effect of vertical shear on tropical cyclone intensity change, J. Atmos. Sci., 53, 2076-2087.

Droegemeier, K. K., Lazarus, S. M. and Davies-Jones, R., 1993, The influence of helicity on numerically simulated convective storms, Mon. Wea. Rev., 121, 2005-2029.

Emanuel, K., 2005, Increasing destructiveness of tropical cyclones over the past 30 years, Nature, 436(7051), 686-688.

Ertel, H., 1942, Ein neuer hydrodynamischer wirbelsatz, Meteor, Z., 59, 271-281.

Fan, K., 2007a, New predictors and a new prediction model for the typhoon frequency over western North Pacific, Science in China (D), 50(9), 1417-1423.

Fan, K., 2007b, North Pacific sea ice cover, a predictor for the western North Pacific typhoon frequency? Science in China (D), 50(8), 1251-1257.

Frank, W. M. and Ritchie, E. A., 1999, Effects of environmental flow upon tropical cyclone structure, Mon. Wea. Rev., 127, 2044-2061.

Frank, W. M. and Ritchie, E. A., 2001, Effects of vertical wind shear on hurricane intensity and structure, Mon. Wea. Rev., 129, 2249-2269.

Gray, W. M., 1968, Global view of the origin of tropical disturbances and storms, Mon. Wea. Rev., 96, 669-700.

Hanley, D. E., Molinari, J. and Keyser, D., 2001, A composite study of the interactions between tropical cyclones and upper tropospheric troughs, Mon. Wea. Rev., 129, 2570-2584.

Jones, D. R. P., Burgess, D. and Foster, M., 1990, Test of helicity as a tornado forecast parameter, Preprints, 16th Conf. on Severe Local Storms, Kanaskis, AB, Canada, Amer. Meteor. Soc., 588-592.

Jones, S. C., 1995, The evolution of vortices in vertical shear: I: Initially barotropic vortices, Quart. J. Roy. Meteor. Soc., 121, 821-851.

Jones, S. C., 2000, The evolution of vortices in vertical shear: III: Baroclinic vortices, Quart. J. Roy. Meteor. Soc., 126, 3161-3185.

Khansalari, S., Farahani, M. M. and Azadi, M., 2011, A study of helicity and helicity flux in the Gonu tropical storm, Iranian Geophysical Society, 5(2),97-115.

Kurgansky, M. V., 2008, Vertical helicity flux in atmospheric vortices as a measure of their intensity, Izvestiya Atmospheric and Oceans Physics, 44, 67-74.

Lajoie F. and Walsh K., 2010, Diagnostic study of the intensity of three tropical cyclones in the Australian Region. Part I: A Synopsis of Observed Features of Tropical Cyclone Kathy (1984), Monthly Weather Review, 138, 3-21.

Lee, W. C. and Wurman, J., 2005, Diagnosed three-dimensional axisymmetric structure of the Mulhall tornado on 3 May 1999, J. Atmos. Sci., 62, 2373-2393.

Lilly, D. K., 1986, The structure, energetic, and propagation of rotating convective storms. Part II: Helicity and storm stabilization, J. Atmos. Sci., 43, 126-140.

McBride, J. L. and Zehr, R., 1981, Observational analysis of tropical cyclone formation, Part II: Comparison of nondeveloping versus developing systems, J. Atmos. Sci., 38, 1132-1151.

Molinari, J. and Vollaro, D., 2008, Extreme helicity and intense convective towers in Hurricane Bonnie, Monthly Weather Review, 136(11), 4355-4372.

Molinari, J. and Vollaro, D., 2010, Rapid intensification of a sheared tropical storm, Mon. Wea. Rev., 138, 3869-3885.

Molinari, J., Romps, D. M., Vollaro, D., and Nguyen, L., 2012, CAPE in tropical cyclones, J. Atmos. Sci., 69(8), 2452-2463.

Nolan, D. and M. McGauley, 2012, Tropical cyclogenesis in wind shear: climatological relationships and physical processes. cyclones: formation, triggers, and control, K. Oouchi and H. Fudeyasu, Eds., Nova Science, in press.

Ramalingeswara Rao, S., Muni Krishna, K. and Bhanu Kumar, O. S. R. U., 2009, Study of tropical cyclone "Fanoos" using MM5 model–a case study, Natural Hazards and Earth System Sciences, 9(1), 43-51.

Rasmussen, E. N. and Blanchard, D. O., 1998, A baseline climatology of sounding-derived supercell and tornado forecast parameters, Wea. Forecasting, 13, 1148-1164.

Raymond, D. J., 1992, Nonlinear balance and potential vorticity thinking at large Rossby number, Quart. J. Roy. Meteor. Soc., 118, 987-1015.

Riehl, R. J., 1948, On the formation of typhoons, J. Meteor., 5, 247-264.

Rossby, C. G., 1940, Planetary flow patterns in the atmosphere, Quart. J. Roy. Meteor. Soc., 66, 68-87.

Shepherd, J. and Knutson, T., 2007, The current debate on the linkage between global warming and hurricanes, Geography Compass, 1(1), 1-24.

Stevenson, S. N., Corbosiero, K. L. and Molinari, J., 2014, The convective evolution and rapid intensification of hurricane Earl (2010), Monthly Weather Review, 12, 4364-4380.

Thompson, R. L., Mead, C. M. and Edwards, R., 2007, Effective storm-relative helicity and bulk shear in supercell thunderstorm environments, Weather and forecasting, 22(1), 102-115.

Titley, D. W. and Elsberry, R. L., 2000, Large intensity changes in tropical cyclones: a case study of super typhoon Flo during TCM-90, Mon. Wea. Rev., 128, 3556-3573.

Webster, P. J., Holland, G. J., Curry, J. A. and Chang, H. R., 2005, Changes in tropical cyclone number, duration, and intensity in a warming environment, Science, 309(5742), 1844-1846.

Weisman, M. L. and Rotunno, R., 2000, The use of vertical wind shear versus helicity in interpreting supercell dynamics, J. Atmos. Sci., 57, 1452-1472.

Zhou, B. T. and Cui, X., 2008, Hadley circulation signal in the tropical cyclone frequency over the western North Pacific, J. Geophys. Res., 113, 1984-2012